

# PHYSICAL REVIEW LETTERS

---

VOLUME 70

17 MAY 1993

NUMBER 20

---

## Global Dynamics and Long-Time Stability in Hamiltonian Systems via Numerical Frequency Analysis

H. S. Dumas

*Department of Mathematical Sciences, University of Cincinnati, Cincinnati, Ohio 45221-0025*

J. Laskar

*Astronomie et Systèmes Dynamiques, Bureau des Longitudes, 77 av. Denfert-Rochereau, 75014 Paris, France*

(Received 18 November 1992)

Frequency analysis is a numerical technique for studying the long-time dynamics of nearly integrable Hamiltonian systems or symplectic maps over large regions of phase space. This technique may be especially useful because of its inherent simplicity, and we demonstrate its effectiveness in studying long-time diffusion of orbits in a simplified but nontrivial accelerator model.

PACS numbers: 03.20.+i, 02.60.-x, 05.45.+b, 29.27.Bd

*I. Introduction.*—Rigorous stability theorems for nearly integrable Hamiltonian systems [e.g., theorems of Kolmogorov-Arnold-Moser (KAM) [1–3] and Nekhoroshev [4] type] have been known for some time; yet in problems of celestial mechanics, plasma confinement, or particle accelerator physics, efforts to obtain realistic stability estimates with such theorems are generally disappointing. Even when stability theorems are carefully tailored to specific problems and proved with computer assistance, the resulting estimates usually agree only roughly with long-time numerical computations. We present here a relatively simple alternative, the frequency analysis method of Laskar [5–7], which may be used to study the long-time dynamics of nearly integrable Hamiltonian systems or symplectic maps over large regions of phase space. In Sec. III we apply this method to a simple accelerator model that was studied extensively by Warnock and Ruth [8,9] using refined techniques for approximating invariant tori. We have chosen this model both as a simple prototype as well as to show how the frequency analysis method compares with the approximate invariant tori techniques. Because of its inherent simplicity, we believe frequency analysis will prove to be a powerful tool in long-time stability studies.

The KAM theorem asserts in part that the nearness to integrability of a conservative system is reflected by the existence, in its phase space, of a family of invari-

ant tori on which integrable behavior persists. Trajectories starting on a torus remain on it thereafter, executing quasiperiodic motion with fixed frequency vector. The family of tori is parametrized over a Cantor set of frequency vectors, while in the ubiquitous gaps of the Cantor set chaotic behavior can—and generically does—occur. For systems with more than 2 degrees of freedom, the chaotic gaps (resonant zones) merge to form an interconnected web passing arbitrarily close to all points in phase space. Arnold [10] constructed a model system with trajectories that wander large distances throughout this web, a phenomenon since known loosely as *Arnold diffusion*. We will use the term “diffusion” to describe the “chaotic transport” of orbits between tori, which may be driven by mechanisms in addition to those (“transition chains, whiskered tori”) described in Arnold’s model. Under rather mild conditions, the speed of this diffusion is known to be exponentially small in the parameter which measures closeness to integrability (Nekhoroshev theory). Unfortunately, despite recent progress [11–13], rigorous mathematical results are not yet refined enough to supplant direct numerical calculation for long-time studies of orbit diffusion.

*II. The frequency analysis method.*—The frequency analysis method grew out of Laskar’s studies of solar system stability [5]. It was successfully applied to simpler multidimensional conservative systems [6,7], and then

used to study the global dynamics of a four-dimensional symplectic map and the diffusion of its orbits between invariant tori [7]. In this respect the method is similar in spirit to the approach taken in [8,9], where the authors use numerical orbit data to compute close approximations to invariant tori. These slightly deformed tori are fixed structures of the model system, and as demonstrated in [8,9], it is possible numerically to find them, to straighten them out, and to interpolate between them to form a toroidal coordinate system (action-angle variables) in which regular (quasiperiodic) motion appears uniformly circular, and weakly chaotic motion stands out as a slight departure. The frequency analysis method also relies on a fixed feature of the model system, but one which is simpler to compute, namely, the frequency vectors associated with each of the invariant tori. Although the frequencies are strictly speaking only defined and fixed on tori, efforts to compute them in resonant regions of phase space yield weakly time-dependent “quasifrequencies” which represent natural interpolations between fixed frequencies.

To understand how the frequency analysis method works, recall that the function  $f : \mathbf{R} \rightarrow \mathbf{C}$  is quasiperiodic in time  $t$  over the  $n$ -torus  $\mathbf{T}^n$  provided there exists a function  $F : \mathbf{R}^n \rightarrow \mathbf{C}$  with unit period in each coordinate, and a fixed frequency vector  $\nu \in \mathbf{R}^n$ , such that  $f$  may be expressed as  $f(t) = F(t\nu)$ . In this case  $f$  may be written as  $f(t) = \sum_{k=-\infty}^{\infty} c_k e^{i\langle m^{(k)}, \nu \rangle t}$ , where the  $c_k$  are complex coefficients with  $|c_k| \rightarrow 0$  and  $\langle m^{(k)}, \nu \rangle$  denotes the integer combination  $m_1^{(k)}\nu_1 + \dots + m_n^{(k)}\nu_n$  of the *fundamental frequencies*  $\{\nu_j\}_{j=1}^n$ . Given a quasiperiodic function  $f$  of the above form, the frequency analysis method finds an approximation  $f'$  of the form  $f'(t) = \sum_{|k| \leq N} c'_k e^{i\langle m^{(k)}, \nu' \rangle t}$ . Although  $f'$  may be used to parametrize close approximations to invariant tori, we also recover close approximations  $\nu'_j$  to the fundamental frequencies  $\nu_j$ , and it is these quantities that will most interest us here.

We now describe briefly how the  $\nu'_j$  are found; more details may be found in Refs. [5–7]. Given a quasiperiodic function  $f$  defined numerically over a certain time interval (say  $[-T, T]$ ), we locate the maximum of  $\Omega(\omega) = \frac{1}{2T} \int_{-T}^T f(t) e^{2\pi i \omega t} \chi(t) dt$  using a quadratic interpolation routine (the accuracy of this process is significantly improved by the presence of an appropriate weighting function  $\chi$ ; cf. [6]). The maximum occurs at one of the fundamental frequencies  $\nu_1$ . We next project  $f$  onto  $e^{2\pi i \nu_1 t}$  to obtain the coefficient  $c_1$ , then subtract this projection from  $f$  and repeat the process to obtain the next fundamental frequency and corresponding coefficient (subsequent projections require a Gram-Schmidt orthogonalization). The process terminates upon reaching the desired number of terms or accuracy, or when the last determined frequency is within the main peaks of any of the previously determined terms. The accuracy of the approximation  $f'$  may be checked by performing a second

frequency analysis on  $f'$ .

For an  $n$  degree of freedom Hamiltonian system (or  $2n$ -dimensional symplectic map), the frequency analysis method establishes a map  $F_T : \mathbf{R}^{2n} \times \mathbf{R} \rightarrow \mathbf{R}^n$   $[(I_0, \phi_0; t) \mapsto \nu]$  which acts on initial conditions  $(I_0, \phi_0) \in \mathbf{R}^{2n}$  for trajectories evolving over the time interval  $[0, t + T]$ . Frequency analysis is performed on these trajectories over the time interval  $[t, t + T]$  to yield the frequency vector  $\nu \in \mathbf{R}^n$ . The important point is that, although  $\nu$  represents a frequency vector only for initial conditions belonging to the set  $\mathcal{A} \subset \mathbf{R}^{2n}$  of initial conditions which give rise to quasiperiodic trajectories, the map  $F_T$  is well defined numerically for all initial conditions, yielding what we call “quasifrequencies” for initial conditions outside  $\mathcal{A}$ . These quasifrequencies vary slightly with the location  $t$  of the time interval  $[t, t + T]$  over which they are evaluated, and their use is described in the next section.

*III. Analysis of a simple accelerator model.*—The advent of increasingly complex particle accelerators operating at energies in the tens of TeV demands new approaches to modeling the long-time dynamics of particle trajectories in storage rings. One such approach was presented in [8,9]; for simplicity and for purposes of comparison, we apply the frequency analysis method to the same problem. Namely, we consider the  $2^{1/2}$  degree of freedom Hamiltonian  $H(I, \phi, s) = \Omega(s) \cdot I + V(I, \phi, s)$  (periodic in  $s$ ) representing transverse betatron oscillations in a nonlinear accelerator lattice. Here  $I = (I_1, I_2)$ ,  $\phi = (\phi_1, \phi_2)$  are action-angle variables of the linear system  $H_L = \Omega(s) \cdot I$ . The nonlinear part  $V$ , due to the presence of sextupole magnets in the lattice, has the form  $V(I, \phi, s) = (1/6)S(s)(x_1^3 - 3x_1x_2^2)$ , where the horizontal and vertical displacements  $x_1, x_2$  of particles in the transverse plane are given in terms of the action-angle variables by  $x_i = [2I_i/\Omega_i(s)]^{1/2} \cos \phi_i$ . For more details and a tabulation of the precise parameter values used in this model, the reader may consult [9]. We note that the actual frequencies at the origin were  $\nu_1 = 1.189735$  and  $\nu_2 = 0.681577$ ; here we use instead  $f_1 = \nu_1 - 1$  and  $f_2 = \nu_2 - 1$ .

Following the formalism established above, we let  $(I_1^0, I_2^0, \phi_1^0, \phi_2^0)$  denote the initial conditions of a trajectory at time  $t = 0$  (in all computations we set  $\phi_1^0 = \phi_2^0 = \pi/2$ ), so that for a given time span  $T$ , the map  $F_T : \mathbf{R}^2 \times \mathbf{R} \rightarrow \mathbf{R}^2$   $[(I_1^0, I_2^0, t) \mapsto (f_1, f_2)]$  returns the two frequencies  $f_1, f_2$  for the corresponding orbit at time  $t$ , computed numerically over the interval  $[t, t + T]$ . If the initial conditions lie on an invariant torus, the frequencies of course remain constant with time  $t$ ; if not, the algorithm returns quasifrequencies which slowly evolve with time. To make use of this map to understand the dynamics, we first consider a fixed value of  $t$ , say  $t = 0$ . This defines a reduced frequency map  $F_T^0 : \mathbf{R}^2 \rightarrow \mathbf{R}^2$   $[(I_1^0, I_2^0) \mapsto (f_1, f_2)]$  which, by KAM theory, should be smooth on the set  $\mathcal{A}$  (smoothness on

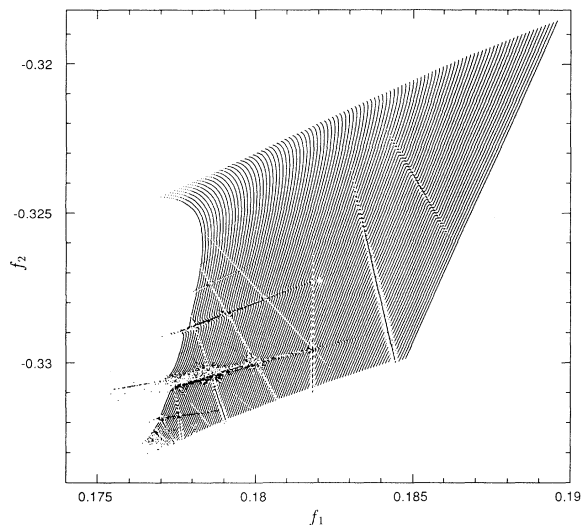


FIG. 1. Image in the frequency plane (“tune space”)  $(f_1, f_2)$  of the square sector  $0 \leq I_1, I_2 \leq 10^{-5}$ , obtained using frequency analysis over 4052 turns.

closed sets is defined in the sense of Whitney; cf. [14]). It is therefore natural to expect diffusion to occur at the singularities of the map  $F_T^0$ . As a first attempt to locate the singularities, we take a square of regularly spaced lines of initial conditions (ICs) in action space  $(I_1, I_2)$  and plot their image under  $F_T^0$  in frequency space  $(f_1, f_2)$ . In Fig. 1 we plot the frequency image of a square sector of 100 regularly spaced lines in action space, each line comprising 500 regularly spaced points (i.e., ICs lie on a rectangular mesh, with spacing  $2 \times 10^{-8}$  in  $I_1$  and  $10^{-7}$  in  $I_2$ ).

If the dynamics of the system were entirely regular (i.e., integrable), we would expect the image of the square sector to be smoothly distorted. Figure 1 shows that this is nearly the case, except near low-order resonances, where relatively abrupt distortions occur (the order of a given resonant line  $m_1 f_1 + m_2 f_2 = m_3$ , where the  $m_i$  are integers, is  $\Sigma_i |m_i|$ ). It should be stressed that the resonant lines appearing in Fig. 1 are not computed beforehand, but instead manifest themselves as irregularities in the frequency map  $F_T^0$ . These irregularities permit us to compute the quantitative effect of resonances on the dynamics of the system.

For some applications, the roughly outlined Arnold web of Fig. 1 might suffice to determine approximately optimal operating frequencies  $(f_1, f_2)$  away from strong resonances. However, small distortions in the frequency map are not visible in Fig. 1, so to obtain a more enhanced view of the resonances, and most important to extract quantitative bounds on the rate of diffusion in unstable regions of frequency space, we use the following simple technique [7].

As mentioned above,  $F_T$  is not quite constant in  $t$  off of the set  $\mathcal{A}$  of ICs for invariant tori. To estimate its

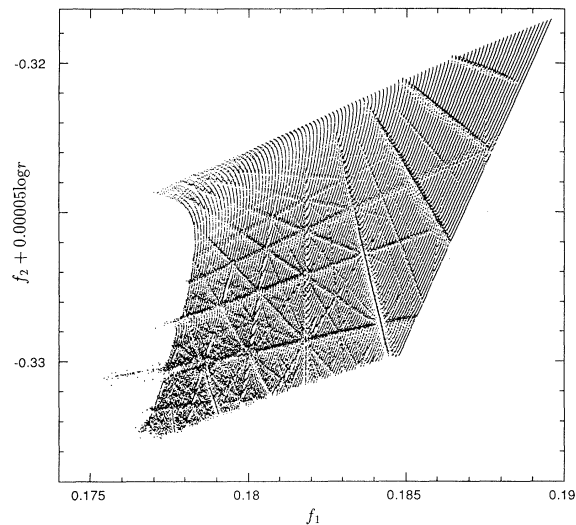


FIG. 2. Transport rates in the frequency plane. The speed and location of local transport phenomena are visualized by plotting  $f_2 + 0.00005 \log(r)$  against  $f_1$  for the same data as in Fig. 1, where  $r$  is the estimated local rate of transport (for  $r$  above a given threshold).

change in  $t$ , we extend the computations used to produce Fig. 1 and thereby compute the numerical derivative  $\frac{1}{T} [F_T(I_1^0, I_2^0, t+T) - F_T(I_1^0, I_2^0, t)]$  [an approximation of  $\frac{\partial F_T}{\partial t}(I_1^0, I_2^0, t)$ ] for the same initial conditions  $(I_1^0, I_2^0)$  used in Fig. 1, and for some fixed time  $t$ . We then take  $r(I_1^0, I_2^0, t) = \max\{|\frac{\partial f_1}{\partial t}(I_1^0, I_2^0, t)|, |\frac{\partial f_2}{\partial t}(I_1^0, I_2^0, t)|\}$  to be an estimate of the maximum speed of transport in frequency space in a small neighborhood of the point  $F_T(I_1^0, I_2^0, t)$ .

In Fig. 2, we display  $r$  in graphic form by adding to the ordinate  $f_2$  of Fig. 1 at each point  $(f_1, f_2)$  the factor  $0.00005 \log(r)$  computed at that point. This yields a striking picture of transport phenomena concentrated along the Arnold web, and shows that, although fast transport is confined to the low-order resonances, significant transport nonetheless takes place throughout an intricate network of resonances, some of very high order. A kind of preimage of the web in action space is shown in Fig. 3, similarly obtained by adding to  $I_2^0$  the factor  $0.04 \log(r)$  computed at  $(I_1^0, I_2^0)$ . Both Figs. 2 and 3 reveal the increasing effect of transport near resonances as one moves away from the origin or its image. We believe Figs. 2 and 3 offer simple but striking pictures of the dynamics of the model system, and that they extend over large enough regions of frequency and action space to indicate the global dynamics of the system.

Finally, we show how knowledge of  $r$  may be used to derive simple but effective bounds on trajectories over time intervals much longer than those available using direct numerical integration. For this purpose, we cover the sector in Fig. 1 with a regular square mesh of size  $1.2 \times 10^{-4}$ . To each point of the mesh we associate an up-

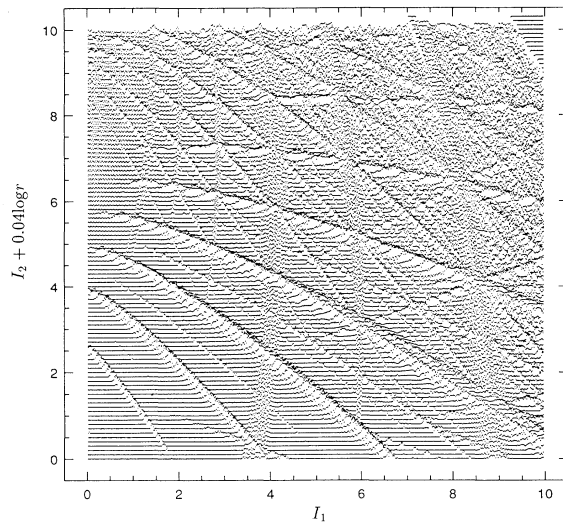


FIG. 3. Transport rates in the action plane ( $I_1, I_2$ ) (units are  $10^{-6}$ ).  $I_2 + 0.04 \log(r)$  is plotted against  $I_1$ , where  $r$  is the estimated transport rate corresponding to the initial condition  $(I_1, I_2)$  in the action plane (for  $r$  above a given threshold).

per bound on the local rate of transport over a mesh-sized square neighborhood of that point; this estimate is simply the largest value of  $r$  computed in that neighborhood. In this way we establish a system of “speed limits,” so to speak, covering the relevant part of the frequency plane, and we ask how far trajectories may be transported over a given time interval subject to these limits. An answer is provided in Fig. 4, where we illustrate “worst case” transport in frequency space. The possible evolution of lines of initial conditions lying along the left and lower edges of the sector is pictured after times corresponding to  $10^7$ ,  $10^8$ ,  $10^9$ , and  $10^{10}$  turns around the accelerator. This simulated evolution is the “worst possible” in the sense that no attempt is made to track the direction of transport; instead it is assumed that transport may occur after the appropriate time interval  $d/2r$  ( $d$  = mesh size,  $r$  = local transport speed), from each occupied point of the mesh to the border of each of its nearest eight neighbors (this is consistent with the way  $r$  is computed). In this way, with increasing time we obtain an expanding region of mesh points necessarily containing all trajectories starting from the original distribution.

This simulation suggests a simple procedure for determining the dynamic aperture of a particular accelerator model. We first decide on a set of unacceptable action values surrounding the origin, i.e., values at which particles are considered to be “lost” by reason of collision with walls of the beam pipe, by the presence of strong resonances, etc. We then use the image of this set in the frequency plane as an initial distribution to simulate worst-case transport over an appropriate time interval (say  $10^8$  turns). The boundary of this evolution, necessarily a closed curve encircling the origin, effectively

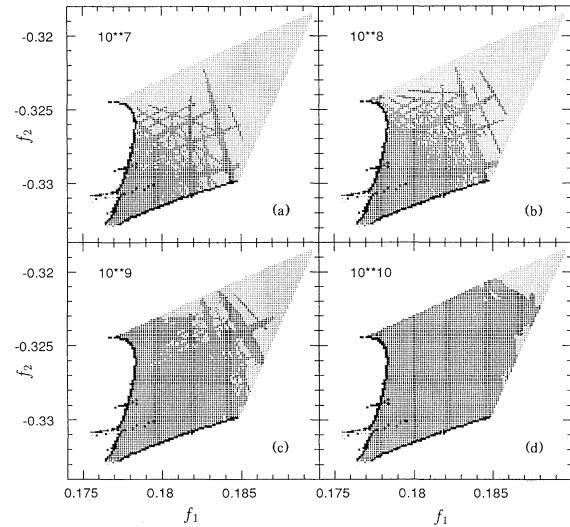


FIG. 4. A simulation, based on frequency analysis, of “worst case” transport in the frequency plane. The frequency sector of Fig. 1 is divided into a mesh; to each point of the mesh is associated an estimate of the maximum rate of transport over a mesh-sized neighborhood. The initial distribution is represented by small crosses, and its evolution after (a)  $10^7$ , (b)  $10^8$ , (c)  $10^9$ , and (d)  $10^{10}$  turns is represented by filled squares. The simulation represents the worst case in the sense that no attempt is made to track the direction of transport, and after a given time the expanding mass of filled squares covers—and necessarily overestimates—the region of the frequency plane accessible to any trajectory starting on the initial distribution.

traces out the dynamic aperture: no particle beginning inside (the preimage in action space of) this curve can reach the set of unacceptable action values in less than  $10^8$  turns.

*IV. Concluding remarks.*—We have presented a simple but effective method for visualizing the global dynamics of nearly integrable systems, as well as for bounding the transport of ensembles of trajectories in frequency space. This suggests a natural way to compute the dynamic aperture for purely Hamiltonian models of accelerator lattices, and we are now at work on computations using a realistic model of the Superconducting Super Collider main ring lattice. We are also formulating a mathematical theory to support our claim that the frequency map  $F_T$  provides a reliable means for computing the transport speed  $r$ . This theory relies on normal forms adapted to resonant regions of phase space, as in Nekhoroshev’s theorem, and should account for possible angle dependence, as well as local variations of quasifrequencies on arbitrarily fine scales of phase space.

We thank Alain Chenciner for helpful discussions concerning the frequency analysis method. One of us (H.S.D.) was supported by the National Science Foundation under Grant No. DMS-9106812, and would also like to thank the Math Departments of the Universities

of Amiens and Paris VII for their hospitality.

- 
- [1] V.I. Arnold, *Russ. Math. Surv.* **18**, 9–36 (1963).
  - [2] A.N. Kolmogorov, in *Stochastic Behavior in Classical and Quantum Hamiltonian Systems*, edited by G. Casati and J. Ford, *Lecture Notes in Physics* Vol. 93 (Springer, Berlin, 1979), pp. 51–54.
  - [3] J.K. Moser, *Nachr. Akad. Wiss. Göttingen, Math. Phys. Kl.* **II**, 1–20 (1962).
  - [4] N.N. Nekhoroshev, *Funct. Anal.* **5**, 338–339 (1971); *Russ. Math. Surv.* **32**, 1–65 (1977); in *Topics in Modern Mathematics, Petrovskii Seminar No. 5*, edited by O.A. Oleinik (Consultants Bureau, London, 1980), pp. 1–58.
  - [5] J. Laskar, *Icarus* **88**, 266–291 (1990).
  - [6] J. Laskar, C. Froeschlé, and A. Celletti, *Physica (Amsterdam)* **56D**, 253–269 (1992).
  - [7] J. Laskar (to be published).
  - [8] R.L. Warnock, *Phys. Rev. Lett.* **66**, 1803–1806 (1991).
  - [9] R.L. Warnock and R.D. Ruth, *Phys. Rev. Lett.* **66**, 990–993 (1991); *Physica (Amsterdam)* **56D**, 188–215 (1992).
  - [10] V.I. Arnold, *Sov. Math. Dokl.* **5**, 581–585 (1964).
  - [11] H.S. Dumas, *Dynamics Reported (New Series)* **2**, 69–115 (1993).
  - [12] P. Lochak, *Russ. Math. Surv.* (to be published).
  - [13] J. Pöschel, *Math. Zeitschr.* (to be published).
  - [14] J. Pöschel, *Commun. Pure Appl. Math.* **25**, 653–695 (1982).